A state-space model of fatigue crack growth*

RAVINDRA PATANKAR, ASOK RAY** and AKHLESH LAKHTAKIA
The Pennsylvania State University, University Park, PA 16802

Abstract. This paper proposes a nonlinear dynamic model of fatigue crack growth in the state-space setting based on the crack closure concept under cyclic stress excitation of variable amplitude and random loading. The model state variables are the crack length and the crack opening stress. The state-space model is capable of capturing the effects of stress overload and underload on crack retardation and acceleration, and the model predictions are in fair agreement with experimental data on the 7075-T6 aluminum alloy. Furthermore, the state-space model recursively computes the crack opening stress via a simple functional relationship and does not require a stacked array of peaks and valleys of stress history for its execution; therefore, savings in both computation time and memory requirement are significant. As such, the state space model is suitable for real-time damage monitoring and control in operating machinery.

Key words: State-space modelling, variable-amplitude load.

1. Introduction

Dynamic modeling of fatigue crack growth has been a topic of intensive research for several decades. A vast majority of fatigue crack growth models have been restricted to constant amplitude stress cycles (Suresh, 1991), where the crack opening stress S^o is assumed to be constant. The fact is that S^o depends on the history of cyclic stresses (Anderson, 1995) and must be cycle-dependent, in general, if the amplitude of stress cycles is not constant. Therefore, for variable-amplitude loading, the history of stress cycles has been taken into consideration in different crack growth models by empirically truncating the cyclic stress history over a finite horizon, i.e., a finite interval of cycles. For example, the crack opening stress in several existing crack growth models, such as FASTRAN-II (Newman, 1992; Newman, 1981)), is calculated based on the stress history over an empirically determined interval of about 300 cycles. In a strain-life-based model, Ray et al. (1994) adopted the rainflow cycle counting method for computing the reference stress (Dowling, 1984) based on the history of finitely many stress cycles. The procedure for selection of the number of cycles in the finite window of stress history varies with the type of load cycles and also the rules employed for cycle counting. Since a finite interval of cycles is an approximation of the semi-infinite time horizon, the accuracy of model prediction is expected to improve as the interval length is increased. In some instances, experimental observations reveal that a short interval of recent stress history is adequate to predict the crack growth rate. However, it is not known precisely how much history should be considered for calculating the crack opening

stress. For variable-amplitude cyclic loading, the procedures for evaluation of crack opening stress in existing crack growth models are usually complicated, computationally intensive, and require storage of a sizable history of stress excitation. This issue has been addressed by Holm et al. (1995) who have formulated an autoregressive (AR) model of crack opening stress in the state-variable setting. Identification of the AR model parameters is restricted to block loading. Apparently, the AR model does not capture the effects of irregular sequence loading (e.g., single-cycle overload and random loading) which is prevalent in many different types of operating machinery.

This paper presents a nonlinear dynamic model of fatigue crack growth in the state-variable setting under cyclic stress excitation of variable amplitude. The model is capable of capturing the effects of block loading, random loading, and irregular sequences including different combinations of single overload and underload. The proposed model, hereafter referred to as the *state-space model*, is formulated based on the crack closure concept where the state variables are the crack length (a) and the crack opening stress (S^o). Although the crack growth equation in the state-space model is similar to that in the FASTRAN-II model (Newman, 1992), the two models use different algorithms for calculating S^o. As such, for a given stress history, the crack length computed by these two models could be different under variable-amplitude cyclic stress but the results are essentially identical under constant amplitude stress. Unlike the existing crack growth models, the state-space model does not require a long history of stress excitation to calculate the crack opening stress and, therefore, savings in both computation time and memory requirement are significant. The effects of the cyclic stress history are captured by a fading memory model where the state equation for crack opening stress is a (piecewise) bilinear difference equation excited by the peaks and valleys of the current stress cycle and the previous stress cycle. This representation adequately captures the phenomena of crack retardation and acceleration resulting from stress overload and underload as well as due to other types of variable-amplitude cyclic stress excitation. The model predictions are in fair agreement with the available experimental data on the 7075-T6 aluminum alloy (Porter, 1972) under various types of variable-amplitude stress excitation including sequence effects.

2. State variable characteristics of the crack opening stress

It is customary in the fracture mechanics literature (for example, Anderson, 1995; Suresh, 1991) to express the dynamics of fatigue crack growth as a derivative da/dN with respect to the number of cycles, which is identical to having the crack length increment $a_{k+1} - a_k$ in the kth cycle. Fatigue crack growth models, reported in technical literature, are usually governed by a first order nonlinear difference equation excited by the maximum applied remote stress ($S_k^{\max}$) and the crack opening stress (S_k^o) in the kth cycle. For example, the crack growth equation in the FASTRAN-II model (Newman, 1992; Newman, 1981) has the following structure

$$a_{k+1} - a_k = h(\Delta K_k^{\text{eff}}) \quad \text{for } k \geqslant 0 \text{ and } a_0 > 0,$$

where the crack length (a_k) at the end of the kth cycle is the state variable; the effective stress intensity factor range; $\Delta K_k^{\text{eff}} := (S_k^{\max} - S_k^o)\sqrt{\pi a_k} F(a_k)$; F is the crack length-dependent correction factor for finite geometry of the specimen. A cycle ranges from a minimum stress to the next immediate minimum stress. If the frequency and shape effects are negligible (e.g., for aluminum and ferrous alloys at room temperature), a stress cycle is defined by the maximum

stress (S^{max}) and the following minimum stress (S^{min}). The nonnegative monotonically increasing function $h(\bullet)$ in (1) can be determined by table-lookup as a function of $\Delta K_k^{\mathrm{eff}}$; details are reported by Newman et al. (1986). This method has been used for generating predictions of both the state-space model and the FASTRAN-II model in Section 4.

As S^o is dependent on the stress history (i.e., the ensemble of peaks S^{max} and valleys S^{min} in the preceding cycles), (1) cannot be readily represented in the state-space setting in its current form. As the objective is to represent the crack growth process by a state-space model, the crack opening stress (S^o) is set as a state variable in addition to the crack length (a). The crack growth process is thus to be modeled in the state-space of dimension 2 (or higher if necessary). In this section, we explore this possibility based on experimental data.

Schijve (1976) collected crack length data for specimens made of 2024-T3 aluminum alloy sheets in simple tension for a constant amplitude load with $S^{\mathrm{max}} = 147\,\mathrm{MPa}$ and $S^{\mathrm{min}} = 98\,\mathrm{MPa}$. The experiments were repeated with the same constant amplitude load with the exception of a single overload cycle with $S^{\mathrm{max}} = 196\,\mathrm{MPa}$ and $S^{\mathrm{min}} = 98\mathrm{MPa}$ when the crack length reached 15 mm. Two curves in each of the three plates in Figure 1 show the respective profiles of crack length, crack opening stress, and crack length increment per cycle, generated from the Schijve data with and without the overload effect. The shaded regions in the two plates of Figure 1 are qualitative due to inexact information on S^o in the experimental data (Schijve, 1976). Recently, Yisheng and Schijve (1995) have observed from experimental data that, following an overload, there is an immediate decrease in S^o followed by a rapid increase and a slow decrease. Similar results were reported earlier by Newman (1982). The sharp transients in decrease and increase of S^o that occur only for a few cycles have no significant bearings on the overall crack growth. The crack growth rate per cycle exhibits a sharp pulse during the overload cycle and then monotonically increases starting from a lower value, as seen in the bottom plate of Figure 1. This experimental observation is in agreement with (1) as we now explain.

The net effect of the single-cycle overload is an abrupt increase in ($S^{\mathrm{max}} - S^o$), resulting in an increase in the crack growth increment in the present cycle. A few cycles after the expiration of the overload, S^o starts decreasing slowly from its increased value as seen in the middle plate of Figure 1. The result is a decrease in ($S^{\mathrm{max}} - S^o$) which causes the crack growth rate to drop. Subsequently, under the constant-amplitude stress, as S^o slowly relaxes back to its original value, crack growth rate also reaches a higher value as seen in Figure 1. The crack growth is therefore retarded due to the fast rise and slow decay of S^o that can be attributed to the crack closure effect.

Now we proceed to make a state-variable representation of the evolution of S^o under variable-amplitude cyclic stress excitation and then augment the crack growth model of Equation (1) with the crack opening stress as an additional state variable. We postulate that the state-space model of crack growth is observable (Vidyasagar, 1992). In other words, the state variables in any given cycle can be determined from the history of measured variables over a finite number of cycles. The crack-length (a) which is one of the two state variables is assumed to be measurable. The other state variable, the crack opening stress S^o, although not necessarily a measurable quantity, can be determined from a finite history of the input (i.e., peaks and valleys of stress excitation) and the output (i.e., crack length measurements) starting from a particular cycle in the past onwards to the current cycle. This concept is analogous to the existing crack growth models that rely on either the crack opening stress or a reference stress based on the history of cyclic stress excitation.
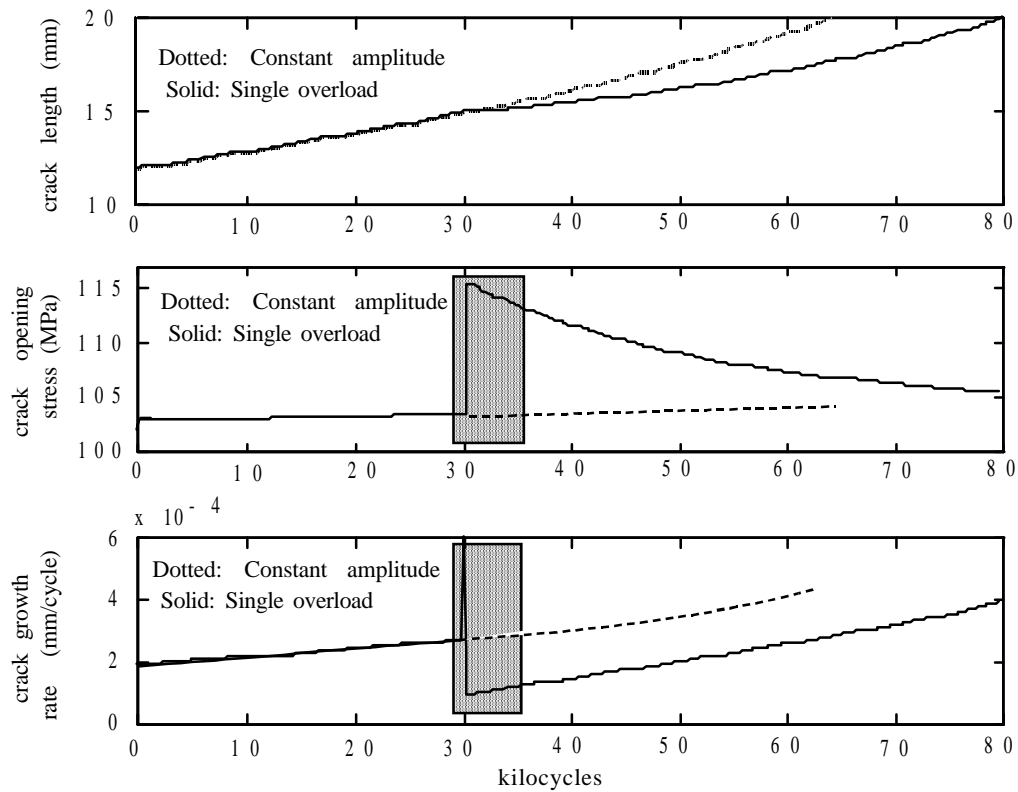
Figure 1. Profiles of crack length, crack opening stress and crack growth rate for overload.

3. Modeling of crack opening stress in the state-variable setting

Experimental observations strongly indicate that the state variable S^o has a fast stable response; i.e., S^o requires a very short time to pick up after the application of overload, which provides a pulse to the crack growth process. Furthermore, an underload (i.e., a negative overload) is observed to have much less significant effects on the crack growth rate and particularly on S^o, as reported by Porter (1972). This behavior suggests that a first order bilinear or nonlinear difference equation is a viable model for describing the dynamic behavior of S^o.

We now proceed to determine the structure of the difference equation and the incorporation of the cyclic stress input therein. To this effect, we first consider the steady-state solution of the difference equation under constant amplitude stress excitation which has been examined by several investigators. The steady-state crack opening stress (S^{oss}) under a constant amplitude cyclic stress is a function of the minimum stress (S^{min}), the maximum stress (S^{max}), the constraint factor α (which is 1 for plane stress and 3 for plane strain) , the specimen geometry, and the flow stress S^{flow} which is the average of the yield strength and the ultimate strength. Such relationships are claimed to be good for most metallic materials. One such semi-empirical relationship has been used in the FASTRAN-II code (Newman, 1992).

To construct the difference equation for S_k^o such that, under different levels of constant-amplitude stress excitation, the forcing function S_k^{oss} at the kth cycle matches the crack opening stress derived from the following empirical relation (Newman, 1984)

$$\frac{S_k^{\text{oss}}}{S_k^{\text{max}}} = A^0 + A^1 R_k + A^2 R_k^2 + A^3 R_k^3, \tag{2}$$

where

$$R_k = S_k^{\text{mod}}/s_k^{\text{max}}, \tag{3}$$

$$S_k^{\text{mod}} = \frac{\alpha S_k^{\text{min}} + S_{k-1}^{\text{min}}}{\alpha + 1}, \tag{4}$$

$$A^0 = (0.825 - 0.34\alpha + 0.05\alpha^2)\left[\cos\left(\frac{\pi}{2}\frac{S_k^{\text{max}}}{S^{\text{flow}}}\right)\right]^{1/\alpha}, \tag{5}$$

$$A^1 = (0.415 - 0.071\alpha)\left(\frac{S_k^{\text{max}}}{S^{\text{flow}}}\right), \tag{6}$$

$$A^2 = \begin{cases} 1 - A^0 - A^1 - A^3 & \text{if } R_k > 0, \\ 0 & \text{if } R_k \leqslant 0, \end{cases} \tag{7}$$

$$A^3 = \begin{cases} 2A^0 + A^1 - 1 & \text{if } R_k > 0, \\ 0 & \text{if } R_k \leqslant 0, \end{cases} \tag{8}$$

and the constraint factor α in (4) is obtained as a function of the instantaneous crack increment in (1).

Now, we propose the following constitutive relation in the form of a (piecewise) bilinear first order difference equation for recursive computation of the crack opening stress (S_k^o) at the completion of the $(k - I)$th cycle

$$S_k^o = \left(\frac{1}{1+\eta}\right)S_{k-1}^o + \left(\frac{\eta}{1+\eta}\right)S_k^{\text{oss}} + \left(\frac{\lambda_k}{1+\eta}\right)(S_k^{\text{oss}} - S_{k-1}^o)\mathfrak{J}(S_k^{\text{oss}} - S_{k-1}^o), \tag{9}$$

$$\eta = \frac{tS^y}{2wE}, \tag{10}$$

where the Heaviside function

$$\mathfrak{J}(x) := \begin{cases} 0 & \text{if } x \leqslant 0 \\ 1 & \text{if } x > 0 \end{cases};$$

S_k^{oss} is calculated from the semi-empirical formula in (2) as if a constant amplitude stress $(S_k^{\text{max}}, S_k^{\text{mod}})$ was applied; the dimensionless parameter η dependents on the specimen thickness t, half-width w, yield strength S^y, and Young's modulus E; and $\lambda_k := (S_k^{\text{max}} - S_k^{\text{mod}})/(S_k^{\text{max}} - S_{k-1}^{\text{min}})$ is the dimensionless, cycle-dependent, pulse scaling factor.

Remark 1. The variable s_k^{oss}, generated from the semi-empirical equation (2), is used to construct the (piecewise bilinear) forcing function to the dynamics of crack opening stress
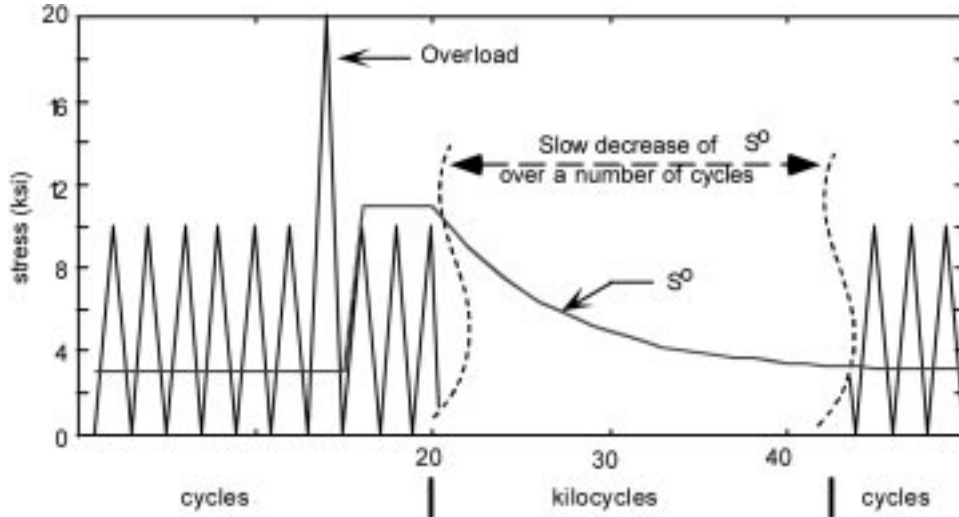
Figure 2. Effect of overload on crack opening stress as predicted by the model.

S_k^o in (9). Under constant amplitude stress excitation, S^{oss} is the steady-state solution of S^o. However, under variable-amplitude stress excitation, S_k^{oss} is different from the instantaneous crack opening stress (S_k^o). ☐

Remark 2. Following an overload cycle, the duration of crack retardation is represented by the dynamics of S^o in the state-space model and hence controlled by the stress-independent parameter η in (9). Physically, this duration depends on the ductility of the material which is dependent on many factors including heat treatment (Schijve, 1976). For example, a lower yield strength produces a smaller η resulting in longer duration of the overload effect. ☐

Remark 3. To include the effects of delay τ (in cycles) at the onset of crack retardation, the crack growth model in (1) can be modified by altering ΔK_k^{eff} as

$$a_{k+1} - a_k = h((S_k^{max} - S_{k-\tau}^o)\sqrt{\pi a_k}F) \text{ with } S_{k-\tau}^o = S_k^{min} \text{ for } k < \tau. \tag{11}$$

In addition, there is a built-in delay of two cycles in the state equations after the application of an overload pulse because the crack growth model, in its present form, is represented by a second order difference equation (see (1) combined with (9)). Since the experimental data may not exactly show the transients of S^o during and immediately after the application of an overload pulse, the effects of an overload pulse could be realized in the model after several cycles onwards. Starting with a higher order difference equation, we reduced the order (i.e., the number of state variables) of the present model to 2 by singular perturbation (Vidyasagar, 1992) based on the experimental data of 7075-T6 Aluminum alloy (Porter, 1972). The possibility of a higher order model to represent longer delays in crack retardation is not precluded for other materials. ☐

3.1. PREDICTION OF OVERLOAD AND UNDERLOAD EFFECTS

Figure 2 shows the effects of a single-cycle overload on S^o as predicted by the model in (9). The model predictions are of similar trend as the experimental data of Yisheng and Schjive (1995) except for the sharp negative spike in S^o immediately after the overload. As stated
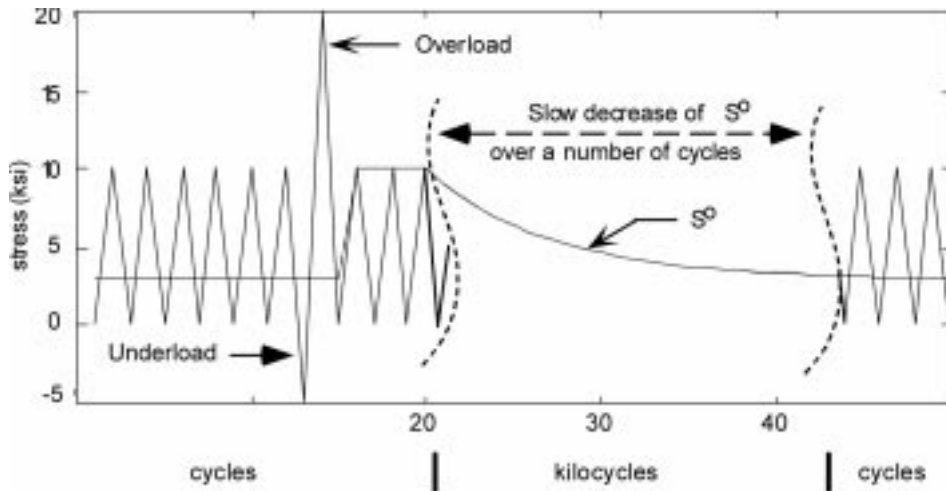
Figure 3. Effect of underload-overload on crack opening stress as predicted by the model.
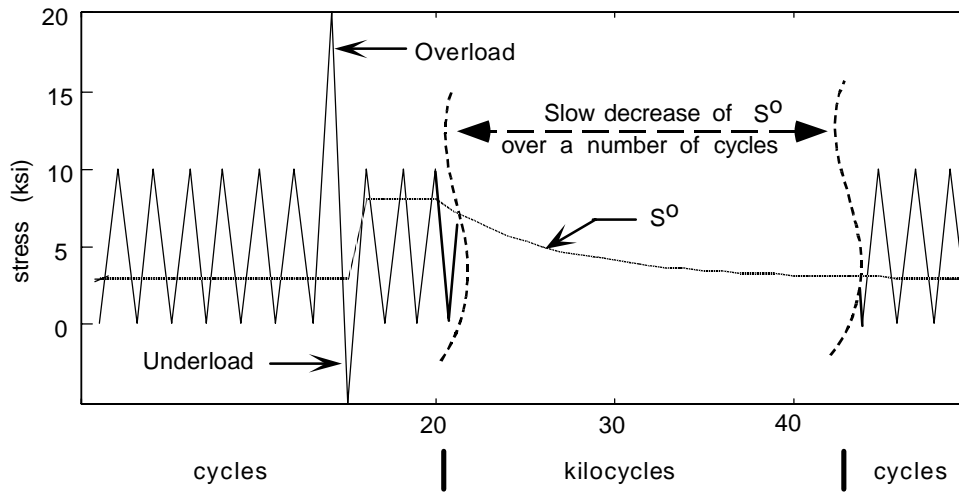
Figure 4. Effect of overload–underload on crack opening stress as predicted by the model.

earlier, the sharp transients of S^o that occur only for a few cycles have no significant bearings on the overall crack growth. Since the dynamics of S^o are described by a first order difference equation, S^o attains a peak value in the cycle following the application of the overload. The positive edge of this resulting pulse is effective whereas, unlike a linear system, the negative edge is rendered ineffective by the Heaviside function $\mathfrak{J}(\cdot)$. When $\mathfrak{J}(\cdot)$ is zero, S^o decreases at a rate decided by the dimensionless parameter η which needs to be identified from test data. The pulse scaling factor is equal to unity, i.e., $\lambda = 1$, for all cycles including the cycle of overload. The amplitude of the input pulse on the right side of (9) depends on the amount of overload, which leads to retarded crack growth unless the overload is too high. In the latter case, the crack damage resulting from the overload itself may dominate the beneficial effects of increased S^o in subsequent cycles.
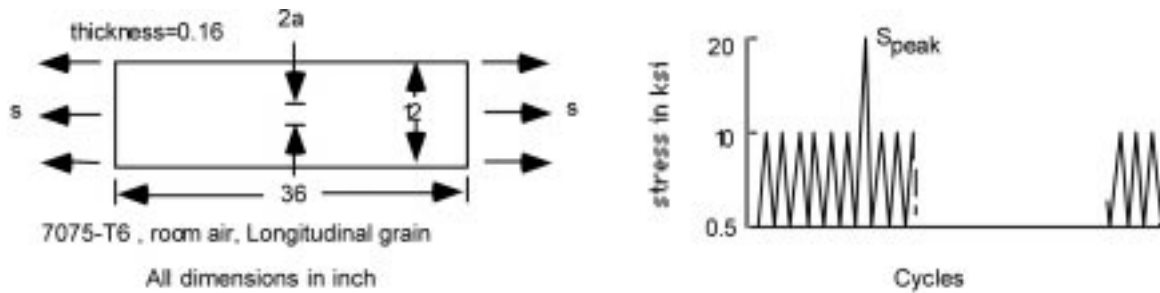
Figure 5. Porter specimen and load for single overload data.
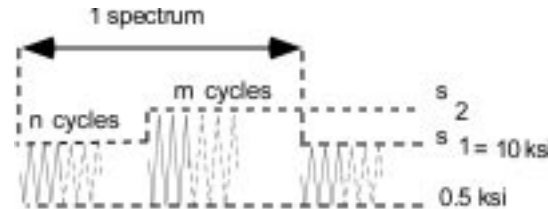
Figure 6. Cyclic stress excitation profile for Porter data.

In contrast to overload, a single-cycle underload causes hardly any change in S^o because the Heaviside function $\mathfrak{J}(\cdot)$ makes the input excitation in (9) largely ineffective for underloads. Figure 3 shows the effect of an underload followed by an overload. The difference between this case and the pure overload case, as modeled in (9), is that the value of the dimensionless pulse scaling factor is less than unity (i.e., $0 < \lambda < 1$) in the cycle of underload-overload and $\lambda = 1$ thereafter.

Figure 4 shows how S^o is affected by an overload immediately followed by an underload. In the overload-underload cycle, $S_k^{\max}$ is identical to that for pure overload but the corresponding $S_k^{\min}$ is smaller. Consequently, S_k^{oss} is smaller for overload-underload than that for pure overload. The pulse scaling term is greater than 1, i.e., $\lambda > 1$, in an overload-underload cycle in contrast to $\lambda > 1$ in a pure overload cycle. The net effect of these two phenomena is that the forcing function (i.e., the sum of the second and third terms on the right-hand side of (9) becomes smaller for overload-underload than that for pure overload. A single-cycle overload retards crack growth more effectively than a similar overload immediately followed by an underload. Therefore, benefits of an overload monotonically diminishes with an increase in the magnitude of the following underload. The overload effects and sequence effects, predicted by the state space model, are in fair agreement to those observed from the experimental test data as we show in Section 4.

3.2. ADVANTAGES OF THE STATE-SPACE MODEL

In this section we compare the state-space model in (9) with the autoregressive (AR) model proposed by Holm et al. (1995). While both models treat crack opening stress (S^o) as a state variable, there are several differences in the structures of their governing equations. For example, the state-space model is piecewise bilinear, whereas the AR model is piecewise linear.

The phenomena of crack acceleration and retardation are captured by the state-space model over a stress cycle via the constant parameter η, and the stress-dependent pulse scaling factor
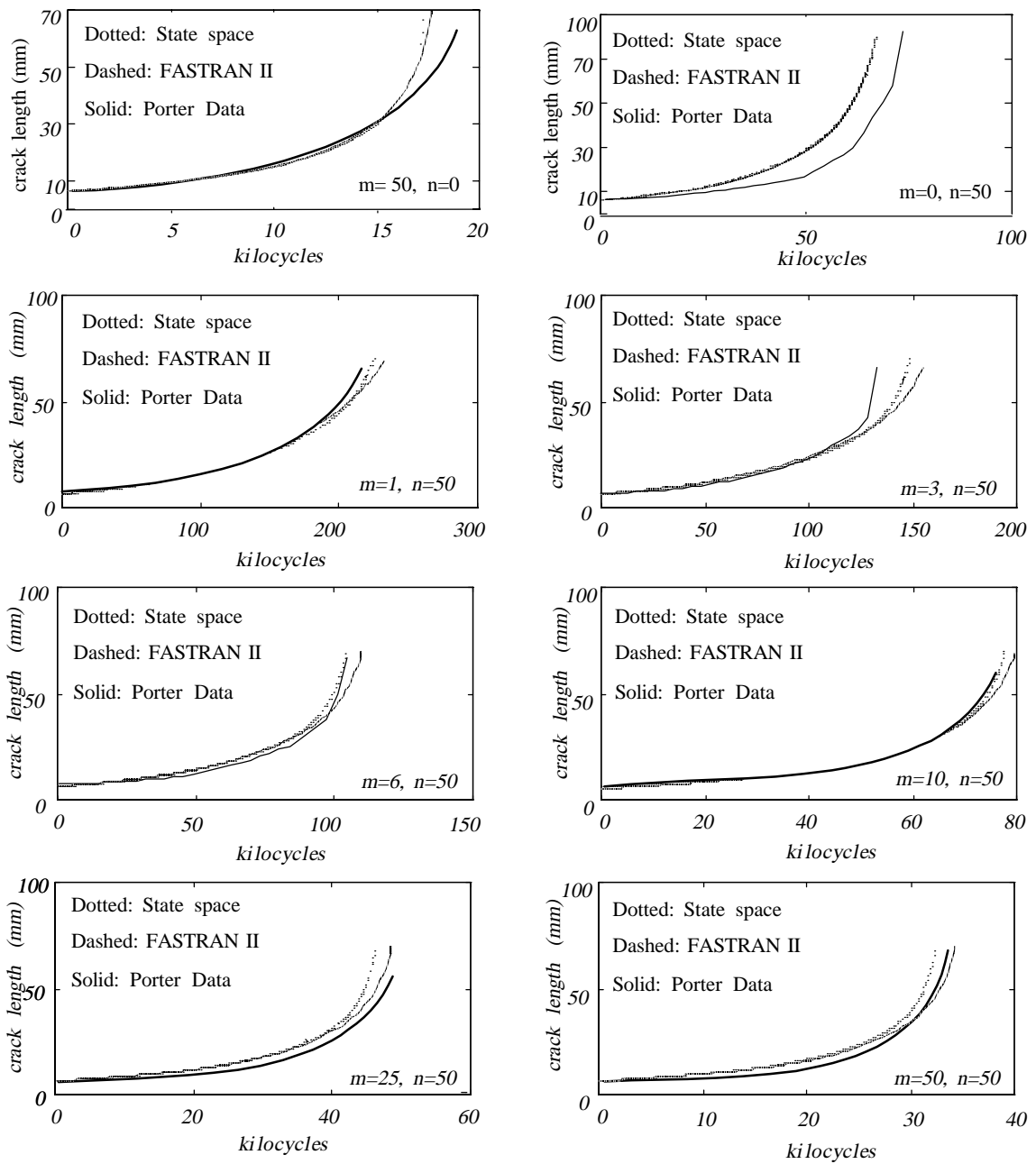
Figure 7. Model validation under block loading: Effect of number of overload cycles.
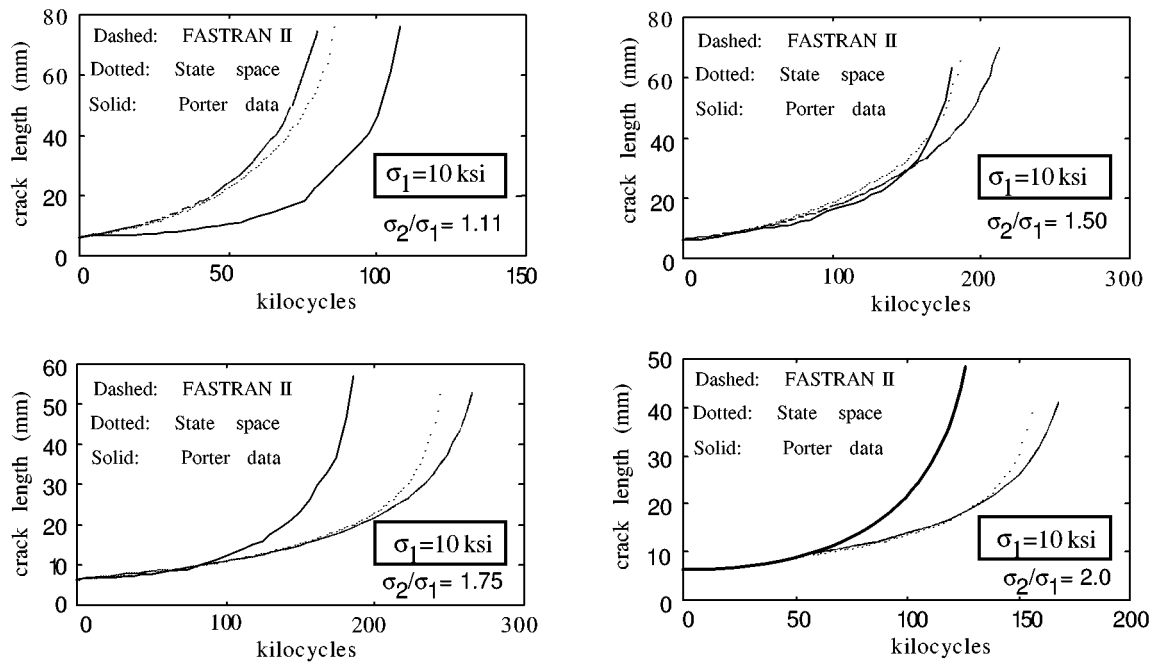
Figure 8. Model validation under different overload amplitudes.

λ, as seen in (9). In contrast, the AR model (Holm et al., 1995) uses (possibly) different constant parameters over the two halves of a cycle to represent the acceleration and retardation effects. The absence of the pulse scaling factor in the AR model is the cause of its failure to capture the single overload effect even with the availability of two parameters. Because of this shortcoming the AR model cannot adequately represent the phenomena of single overload, irregular load sequences, and random loads. Unlike the state-space model, the parameter identification in the AR model is restricted to block loading. The two parameters in the AR model may be required to differ significantly to represent fast acceleration and slow retardation of crack length. This may lead to physically unrealistic values of the crack opening stress (S^o) under irregular load sequences. If the two parameters are made identical as suggested by Holm et al. (1995), the AR model may generate reasonable values of S^o. However, the resulting rates of S^o will be similar under acceleration and retardation which contradicts experimental observations (Schijve, 1976). In addition, having these parameters to be identical may lead to conservative estimation of crack growth.

4. Model validation and discussion of results

Let us now compare the state-space model predictions with the available experimental data on 7075-T6 aluminum alloy specimens under variable-amplitude cyclic stress excitation. The implication of sequence effects is also explained from the perspectives of the state-space formulation of the crack opening stress in (9).
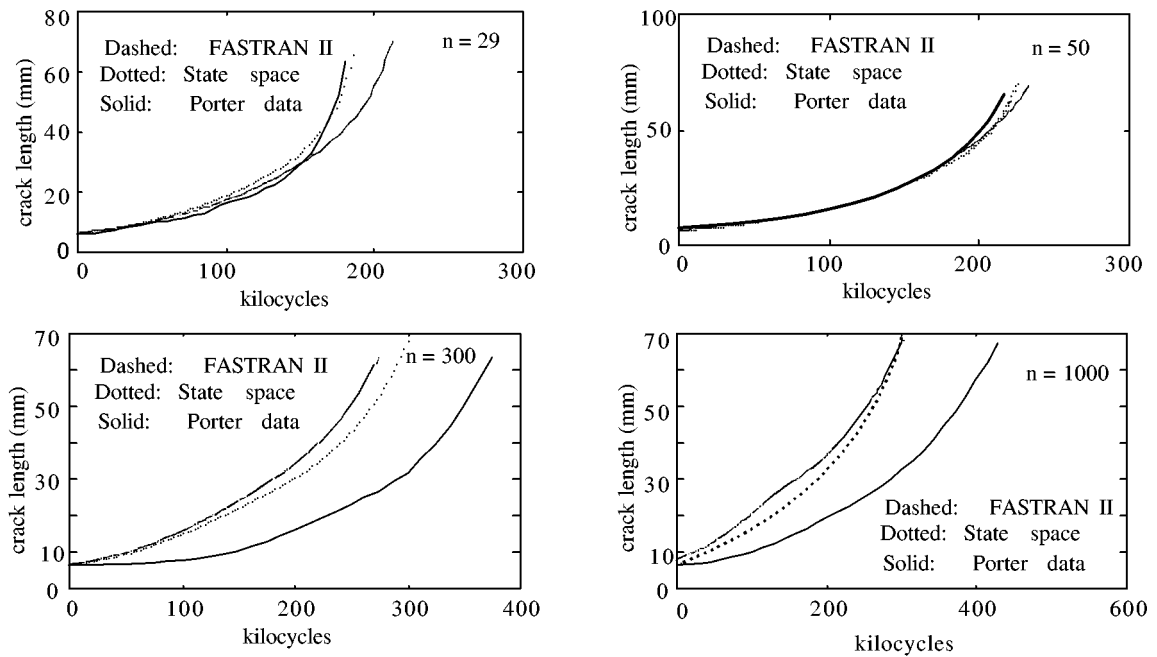
Figure 9. Model validation under different overload spacing.

4.1. VALIDATION OF MODEL RESULTS WITH EXPERIMENTAL DATA

Porter (1972) collected fatigue crack data under tensile load for specimens made of 7075-T6 aluminum alloy sheets. Figure 5 shows a schematic of the Porter specimen for which the constraint factor α in (4) varies between 1.0 and 1.8 depending on the instantaneous crack increment in (1) (see p. 62, Newman, 1992). The dimensionless parameter η given by (10) was $\sim 10^{-4}$, for Porter's specimen. The load profile for this set is shown in Figure 5. Since η is stress-independent, this specific value of η has been used for all identical specimens under different loading conditions in order to validate the state-space model by comparison with the rest of Porter data.

Figure 6 illustrates a profile of block loading applied to the Porter specimens to collect data that are used to validate the crack growth model constructed by combining (1)–(10). Figure 7 shows a comparison of the state-space model predictions with actual experimental data and the predictions of FASTRAN-II model (which calculates the crack opening stress S^o in a different way). The curves in each plate of Figure 7 are generated with the parameter $n = 50$ and the peak stress of overload $\sigma_2 = 15$ ksi at different values of m in the load spectrum of Figure 6. The state-space model and the FASTRAN-II model produce essentially identical results under constant amplitude cyclic stresses because the procedure for calculating s^{oss} is the same for both. For variable-amplitude cyclic stresses, the state-space model predictions are very close to the experimental data and predictions of the FASTRAN-II model, as seen in Figure 7. Both models are again compared with experimental data for different amplitudes of overload in Figure 8 for $m = 1, n = 29$, and different overload stress ratios σ_2/σ_1; as well as for different overload spacing in Figure 9 for $m = 1$, and peak overload stress $\sigma_2 = 15$ ksi, and different n in the load spectrum of Figure 6. The plots in Figures 8 and 9 indicate that the accuracy of the
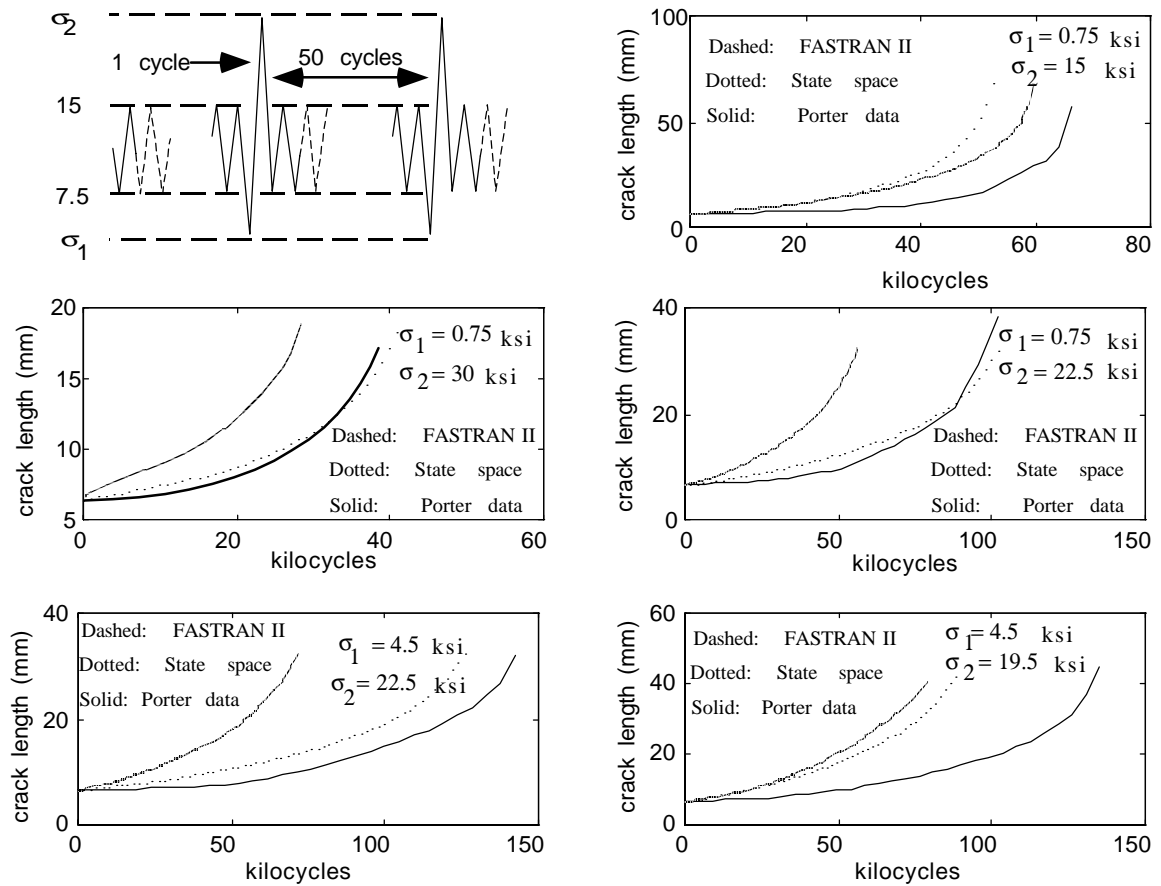
Figure 10. Model validation under sequence effect (underload-overload).

state-space model relative to the experimental data is comparable to that of the FASTRAN-II model. The sequence effects are also captured by the state-space model as seen in Figures 10 and 11.

The agreement of model predictions with experimental data in Figures 7 to 11 strongly supports the hypothesis that the crack opening stress is a state variable, thus validating the foundations of the state-space model.

4.2. COMPARISON OF COMPUTATION TIME

A comparison of the computation time for the state-space model and the FASTRAN-II model reveals that the former is faster and, therefore, more economical to execute in real time. The state-space model recursively computes S_k^o with $S_k^{\max}$, $S_k^{\min}$, and $S_{k-1}^{\min}$ as inputs, as seen in (9). This implies the crack opening stress in the present cycle is obtained as a simple algebraic function of the maximum and minimum stress excitation in the present cycle as well as the minimum stress excitation and the crack opening stress in the immediately preceding cycle.
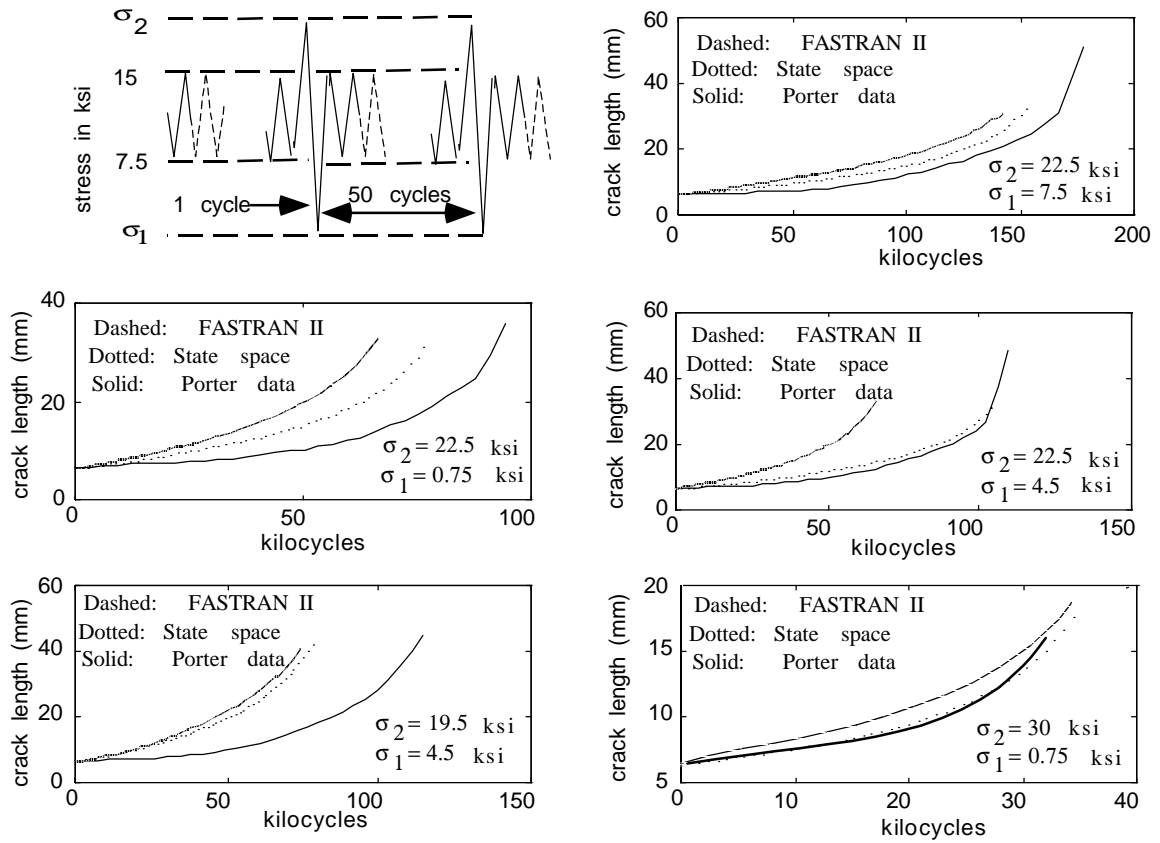
Figure 11. Model validation under sequence effect (overload-underload).

Table 1. Computer execution time in minutes: seconds on an SGI Indy workstation

Load description	State-space model	FASTRAN-II model
1000 cycles 10 ksi and 1 cycle 15 ksi, $S^{min} = 0.5$ ksi	1:20	3:19
300 cycles 10 ksi and 1 cycle 15 ksi, $S^{min} = 0.5$ ksi	1:14	3:27
50 cycles 10 ksi and 1 cycle 15 ksi, $S^{min} = 0.5$ ksi	0:54	1:58
Overload/underload 22.5/4.5 ksi, constant amplitude 15-7.5 ksi	0:28	2:26

In contrast, the FASTRAN-II model computes the crack opening stress as a function of contact stresses and crack opening displacements based on the stress history. Consequently, both computer execution time and memory requirement of the proposed state-space model is significantly smaller than those of the FASTRAN-II model. Table 1 lists typical computation times required on an SGI Indy workstation for calculation of crack growth under variable-amplitude cyclic stress excitation.

5. Summary and conclusions

A fatigue crack growth model has been formulated in the state-space setting based on the crack closure concept where the state variables are the crack length (a) and the crack opening stress (S^o). The effects of the cyclic stress history are represented by a fading memory model where the state equation for crack opening stress is a (piecewise) bilinear difference equation excited by the peaks and valleys of the current stress cycle and the previous stress cycle. The state-space model captures pertinent traits of the crack growth process under variable-amplitude cyclic stresses that have been observed by other researchers and are listed by Schijve (1976).

Unlike the existing crack growth models, the state-space model does not require a long history of stress excitation to calculate the crack opening stress. Specifically, the state space enjoys the following advantages over many crack growth models:

- Smaller execution time and computer memory requirements as needed for real-time damage monitoring and control.
- Compatibility with other state-space models of plant dynamics (e.g., aircraft flight systems and rocket engine systems) and structural dynamics of critical components as needed for synthesis of life extending control systems (Ray et al., 1994).

The structure of the fatigue crack growth equation in the state-space model is similar to that in the FASTRAN-II model (Newman, 1992), but the algorithm for calculation of the crack opening stress is different. Both models are shown to be of comparable accuracy and are in fairly close agreement with experimental data of 7075-T6 Aluminum alloy under different types of variable-amplitude cyclic stress excitation.

Acknowledgements

References

Anderson, T.L. (1995). *Fracture Mechanics*, CRC Press, Boca Raton, Florida.

Dowling, N.E. (1983). Fatigue life prediction for complex load versus time histories. *ASME Journal of Engineering Materials and Technology, Trans. ASME* **105**, 206–214.

Holm, S., Josefson, B.L., de Mare, J. and Svensson, T. (1995). Prediction fatigue life based on level crossings and a state variable, *Fatigue and Fracture of Engineering Materials* **18**(10), 1089–1100.

Newman, J.C. (1981). *A Crack-Closure Model for Predicting Fatigue Crack Growth under Aircraft Loading*, Methods and Models for Predicting Fatigue Crack Growth under Random Loading, ASTM STP **748**, 53–84.

Newman, J.C. (1982). Prediction of fatigue crack growth under variable amplitude and spectrum loading using a closure model, *Design of Fatigue and Fracture Resistant Structures*, ASTM STP **761**, 255–277.

Newman, Jr., J.C. (1984). A crack opening stress equation for fatigue crack growth, *International Journal of Fracture* **24**, R131–R135.

Newman, J.C., Swain, M.H. and Phillips, E.P. (1986). An assessment of the small-crack effect for 2024-T3 aluminum alloy. In: *Small Fatigue Cracks*, (Edited by R.O. Ritchie and J. Lankford).

Newman, Jr., J.C. (1992). FASTRAN-II – A fatigue crack growth structural analysis program, *NASA Technical Memorandum 104159*, Langley Research Center.

Porter, T.R. (1972). Method of analysis and prediction for variable amplitude fatigue crack growth, *Engineering Fracture Mechanics* **4**, 717–736.

Ray, A., Wu, M-K, Carpino, M. and Lorenzo, C.F. (1994). Damage mitigating control of mechanical systems: Part I and II, *ASME Journal of Dynamic Systems, Measurements and Control* **116**(3), 437–455.

Schijve, J. (1976). *Observations on the Prediction of Fatigue Crack Growth Propagation Under Variable-Amplitude Loading*, Fatigue Crack Growth Under Spectrum Loads, ASTM STP 595, pp. 3–23.

Sharpe, W.N., Jr., Corbly, D.M. and Grandt, A.F., Jr. (1976). *Effects of Rest Time on Fatigue Crack Retardation and Observation of Crack Closure*, Fatigue Crack Growth Under Spectrum Loads, ASTM STP 595, pp. 61–77.

Suresh, S. (1991). *Fatigue of Materials*, Cambridge University Press, Cambridge, UK.

Vidyasagar, M. (1992). *Nonlinear Systems Analysis*, 2nd ed., Prentice Hall, Englewood Cliffs, NJ.

Yisheng, W. and Schijve, J. (1995). Fatigue crack closure measurements on 2024-T3 sheet specimens, *Fatigue and Fracture of Engineering Materials and Structures* **18**(9), 917–921.